Generation of DEMs of the Syrian coastal mountains from Sentinel-1 data

Muhannad Hammad[1]– Boudewijn Van Leeuwen[2] – László Mucsi[3]

[1] PhD student, University of Szeged Department of Physical Geography and Geoinformatics, muhannad@geo.u-szeged.hu;

[2] assistant Professor, University of Szeged Department of Physical Geography and Geoinformatics, leeuwen@geo.u-szeged.hu;

[3] associate Professor, University of Szeged Department of Physical Geography and Geoinformatics, mucsi@geo.u-szeged.hu;

Abstract: Digital elevation model (DEM) is a three-dimensional digital model showing the physical and the topographic situation of the earth's surface using an appropriate interpolation method. DEMs are used in many fields such as natural resources management, geo-hazard, hydrology analysis, archaeology... etc. Digital elevation models have been obtained using traditional method of digitizing contour maps. Recently, digital elevation model data can be generated by processing of stereo optical satellite data, radar data and lidar data using special remote sensing techniques. This paper explains the method used to generate a DEM of the Syrian coastal mountains from Sentinel-1 data, Interferometry Wide Swath mode in ascending pass direction and VV polarisation. The error of elevation was computed and the maximum error was equal to 2.74 m.

Introduction

Modern radar technologies like Synthetic Apature Radar (SAR) and Interferometry SAR (InSAR) result in an increased use of digital elevation models for visualization of the earth's surface. Also, because they have some special advantages, such as fast, high precision, and working without the limitation of time and climates (SANSOSTI ET AL. 2014).

SAR uses amplitude and phase differences between the sent signal and recieved signal. InSAR measures the radiation travel path accurately because it is coherent, and travel path variations as a function of the satellite position and time of acquisition allow for the generation of digital elevation models (DEM) and measurement of centimeter scale surface deformations of the terrain (FERRETTI ET AL. 2007).

Many different software packages exist to process SAR data, and each providing a special set of algorithms combinations. Nowadays many open source solutions are available, which can be downloaded free of chage from the internet (GRANDIN R. 2015).

In 2014, the Sentinel-1A satellite was launched by the European Space Agency (ESA). Its twin satellite, the Sentinel-1B launched in 2016 carries an identical instrument to acquire SAR images. Compared with its predecessors such as ERS-1/2 SAR and ENVISAT ASAR, its revisit time and coverage have dramatically improved

(TORRES ET AL. 2012). The satellites carry a C-band SAR sensor which offers medium and high-resolution imagery in all weather conditions and provides a high level of service reliability with near-real-time delivery of data within 24 hours (RUCCIA A. ET AL. 2012).

Material and methods

In this paper, Sentinel-1 data, single look complex, interferometry wide swath mode in ascending pass direction and with VV polarisation for two different acquisition dates 06/10/2014 and 18/10/2014 were co-registered as master and slave respectively. These images with a 40.6 m perpendicular and a 12 days temporary baseline (*Table 1*) and a coherence better than 95 % were used to generate an interferogram for the study area using the ESA's SNAP 5.0.2 software (*Fig. 1*).

After flattening the generation interferogram and applying the deburst process to seamlessly join all burst data into one single image (NIKOLAKOPOULOS K. 2015), goldstein phase filtering of the interferogram phase was applied to remove the phase noise in the generated interferogram, which is directly related to interferometric coherence and the look number of the interferogram (LI ET AL. 2008).

Then, with the help of SNAPHU, the statistical-cost network-flow algorithm, the interferogram phase was unwrapped to recover the integer number of cycles n to be added to the wrapped phase φ so that the unambiguous phase value ψ can be finally obtained for each image pixel from this equation (FERRETTI ET AL. 2007):

$$\psi = \varphi + 2\pi * n$$

Finally, the relative values of the unwrapped phase were converted into absolute elevation values, and at the end a digital elevation model (DEM) was produced (*Fig. 2*).
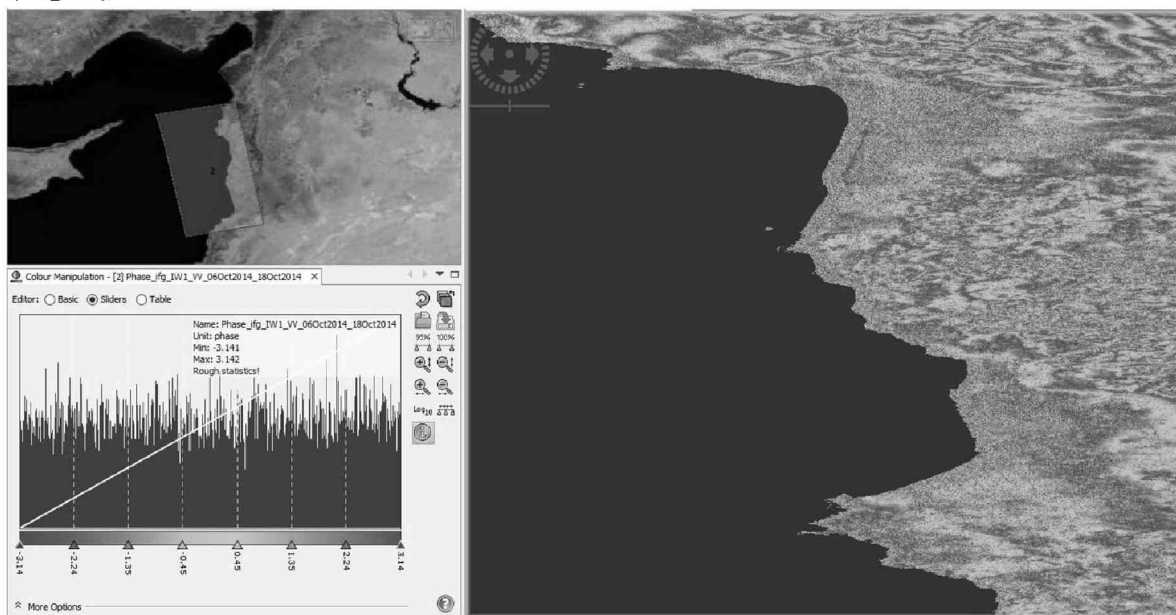

Figure 1. Interferogram for the Syrian coastal mountains

Table 1. Overview of used Sentinel-1 data

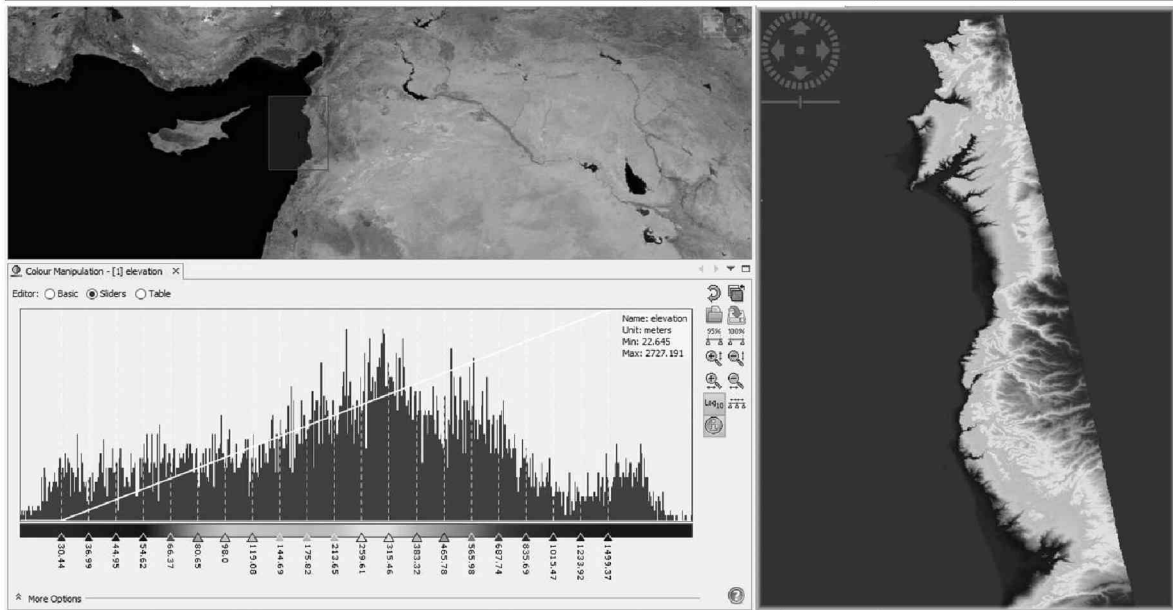| File Name	Mst/Slv	Acquisition	Orbit	Bperp [m]	Btemp [days]	Modeled Coherence
S1A_IW_ SLC_1SDV_20141006	Master	06Oct2014	2711	0.00	0.00	1.00
S1A_IW_ SLC_1SDV_20141018	Slave	18Oct2014	2886	-40.60	-12.00	0.96

Figure 2. Digital Elevation Module (DEM) for the Syrian coastal mountains
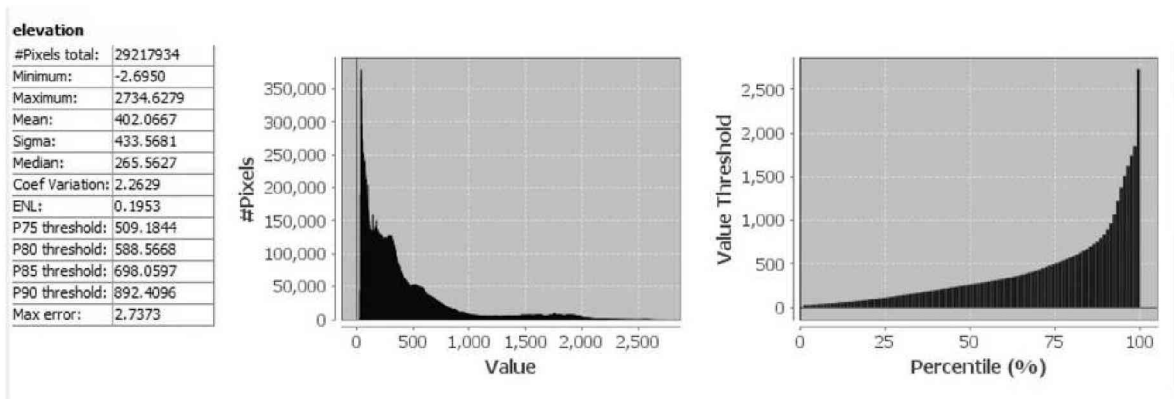

Figure 3. The Maximum error of the elevation values in the generated DEM

Results

A digital elevation model (DEM) for more than 2000 km² area along the Syrian and part of Lebanese coastal mountains was produced with pixel spacing [2.3 x 14] m [range x azimuth]. The highest elevation in the area was 2734 m in the Lebanese part, while the highest elevation in the Syrian part was 1582 m. Statistic analysis available in SNAP software was applied on the generated DEM. The coefficient variation was 2.26, and the maximum error was 2,74 m (*Fig. 3*).
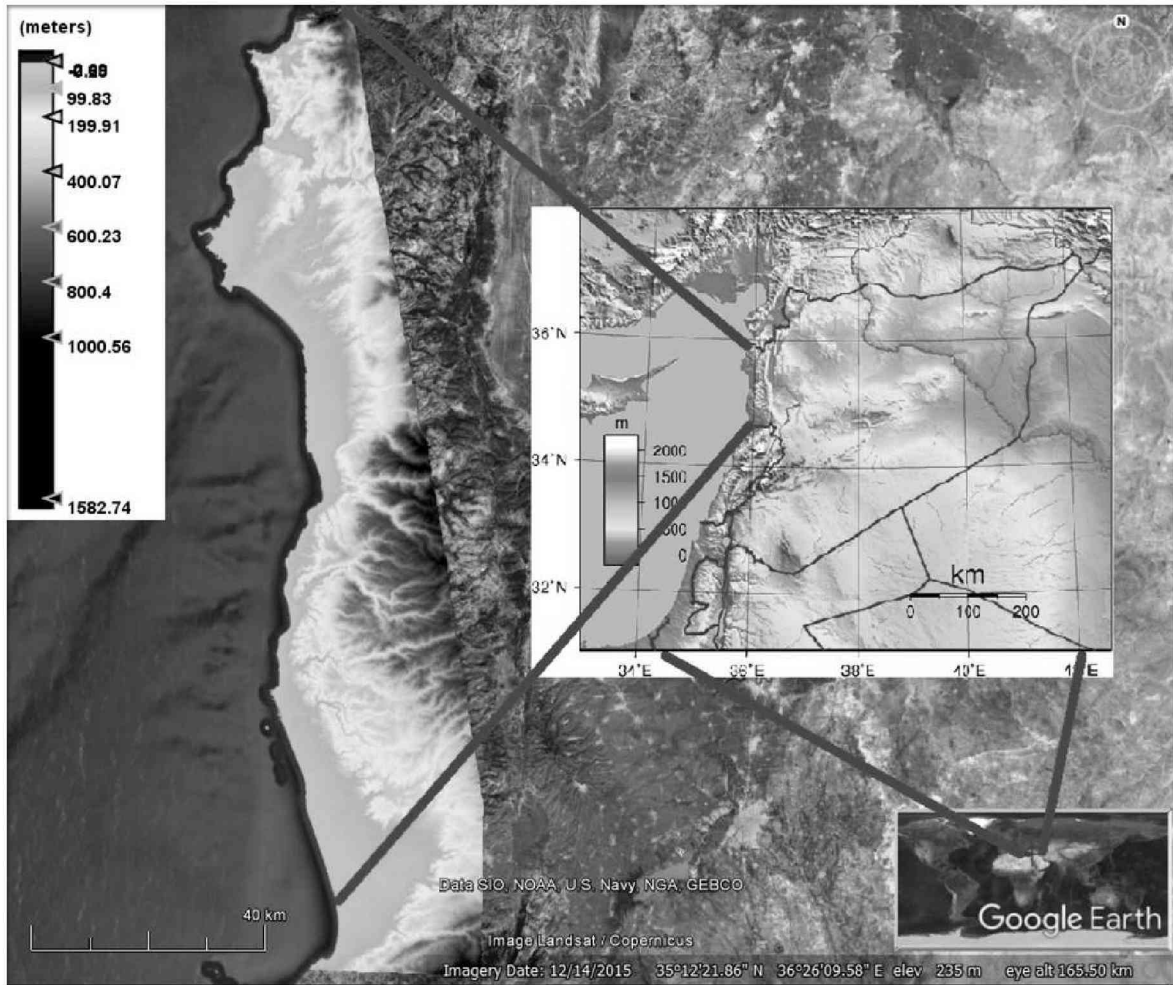
135

Figure 4. The generated digital elevation model DEM on GoogleEarth image

The digital elevation model was vizualized on top of a high resolution satellite image in GoogleEarth to evaluate its' accurcy. In (*Fig. 4*), Arwad, the only island in Syria, is showen in the south part of the syrian coast beside Tartous city even its' maximum elevation is almost 10 m.

Conclusion

The paper confirmed the abilty of free Sentinel-1 radar data to generate high resolution digital elevation modules using freely available open-source software. It is useful and effective specially in the inaccessible areas such as in Syria. The availability of Sentinel-1 radar data for the generation of more accurate DEMs and the measurements of centimetric surface deformations of the terrain is very promising for future applications.

136

References

FERRETTI A. – GUARNIERI A. – PRATI C. – ROCCA F. – MASSONNET D. (2007): InSAR Principles: Guidelines for SAR interferometry processing and interpretation, ESA Publications.

GRANDIN R. (2015): Interferometric Processing of SLC Sentinel-1 TOPS Data, Proceedings of ESA Fringe 2015 Workshop.

LI Z. – DINGA X. – HUANGA C. – ZHUB J. – CHENA Y. (2008): Improved filtering parameter determination for the Goldstein radar interferogram filter, Journal of Photogrammetry & Remote Sensing 63 (2008) pp. 621–634.

NIKOLAKOPOULOS K. – KYRIOU A. (2015): Preliminary results of using Sentinel-1 SAR data for DSM generation, European Journal of Geography 6(3): 52–68.

RUCCIA A. – FERRETTI A. – MONTI GUARNIERIA A. – ROCCA F. (2012): Sentinel 1 SAR interferometry applications: The outlook for sub millimeter measurements, Remote Sensing of Environment 120, pp. 156–163.

SANSOSTI E. – BERARDINO P. – BONANO M. – CALÒ F. – CASTALDO R. – CASU F. –MANUNTA M. – MANZO M. – PEPE A. – PEPE S. – SOLARO G. – TIZZANI P. – ZENI G. – LANARI R. (2014): How second generation SAR systems are impacting the analysis of ground deformation, International Journal of Applied Earth Observation and Geoinformation 28, pp. 1–11.

TORRES R. – SNOEIJ P. – GEUDTNER D. – BIBBY D. – DAVIDSON M.. – ATTEMA E. – ROSTAN F. (2012): GMES Sentinel-1 mission. Remote Sensing of Environment, 120, pp. 9–24.

137